JACS
JOURNAL OF THE AMERICAN CHEMICAL SOCIETY
pubs.acs.org/JACS
Article

Selective Targeting of Guanine-Vacancy-Bearing G-Quadruplexes by G-Quartet Complementation and Stabilization with a Guanine–Peptide Conjugate

Yi-de He, Ke-wei Zheng,* Cui-jiao Wen, Xin-min Li, Jia-yuan Gong, Yu-hua Hao, Yong Zhao, and Zheng Tan*

Cite This: J. Am. Chem. Soc. 2020, 142, 11394–11403
Read Online
ACCESS | Metrics & More | Article Recommendations | Supporting Information

ABSTRACT: Stabilization of G-quadruplexes (G4s) formed in guanine-rich (G-rich) nucleic acids by small-molecule ligands has been extensively explored as a therapeutic approach for diseases such as cancer. Finding ligands with sufficient affinity and specificity toward G4s remains a challenge, and many ligands reported seemed to compromise between the two features. To cope with this challenge, we focused on targeting a particular type of G4s, i.e., the G-vacancy-bearing G-quadruplexes (GVBQs), by taking a structure complementation strategy to enhance both affinity and selectivity. In this approach, a G-quadruplex-binding peptide RHAU23 is guided toward a GVBQ by a guanine moiety covalently linked to the peptide. The filling-in of the vacancy in a GVBQ by the guanine ensures an exclusive recognition of GVBQ. Moreover, the synergy between the RHAU23 and the guanine dramatically improves both the affinity toward and stabilization of the GVBQ. Targeting a GVBQ in DNA by this bifunctional peptide strongly suppresses *in vitro* replication. This study demonstrates a novel and promising alternative targeting strategy to a distinctive panel of G4s that are as abundant as the canonical ones in the human genome.

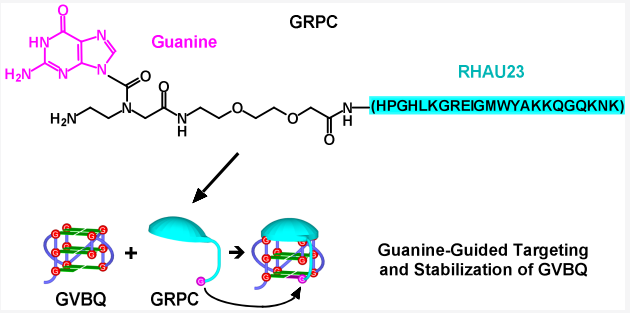

INTRODUCTION

G-quadruplexes (G4s), four-stranded structures formed by guanine-rich nucleic acids, are important drug targets because of their implication in physiological and pathological processes.[1−3] Putative G-quadruplex forming sequences (PQSs) are enriched around transcription start sites[4−8] and can form G4s in response to transcription.[8−15] In the past two decades, there has been tremendous enthusiasm for exploring G4-binding ligands as therapeutic drugs for diseases such as cancer.[16,17] So far, nearly 1000 G4 ligands, which are all small molecules, have been documented.[18] One of the challenges with the small molecule ligands is the compromise between specificity and affinity. To enhance the binding affinity to G4s that are negatively charged, positively charged ligands are favored by electrostatic attraction. On the other hand, however, the positive change leads to nonspecific binding to non-G4 nucleic acids as well as proteins. For many characterized ligands, their dissociation constant (K_d) values are among several tens of nM to several tens of μM with a few folds or up to 100 times selectivity over duplex structures.[19]

In the human genome, there exist "imperfect" G4s with a vacancy[20−23] or bulge.[24] We thought the "imperfect" guanine-vacancy-bearing G4s (GVBQ) might be promising target candidates to enhance both affinity and selectivity without compromising between them. Our previous computational searching showed that such GVBQ motifs are nearly as abundant as the "perfect" canonical G4s,[21] and recent studies have demonstrated their regulatory role in gene expression and interactions with guanine metabolites.[26] The presence of a G-vacancy in a GVBQ can serve as an additional binding site that is not present in other forms of structures. Upon binding to a DNA G4, a ligand forms a complex with the target and interferes with DNA metabolism by two distinct mechanisms.[27] First, it may displace G4-binding proteins from the G4 or prevent the binding of a protein to the G4.[28,29] Second, it reinforces the physical obstacle of the G4 that has to be resolved by helicase in any DNA-reading activities such as transcription and replication.[25,30,31] In the latter case, the impact of a G4 will depend on the stability increment of the G4/ligand complex. Since GVBQs are much less stable than the canonical G4s due to the presence of an incomplete guanine quartet,[21] targeting GVBQs may result in a greater

Received: January 20, 2020
Published: June 3, 2020

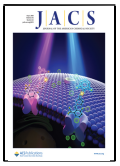

increase in the stability of the GVBQ/ligand complexes relative to the GVBQs and hence leads to greater potency.

Based on such anticipation, we synthesized a bifunctional guanine−RHAU23 peptide conjugate (GRPC) to target the GVBQs as an alternative to small molecules. This conjugate consisted of a guanine moiety and a 23-aa G4-binding domain (RHAU23) from the RHAU protein,[32] an RNA helicase able to bind and unwind G4 structures. The guanine moiety could fill into the G-vacancy in a GVBQ to guide the binding of the RHAU23 toward the GVBQs. With a synergy of the two binding activities from the two functional units, this guided targeting resulted in a superior specificity to and stabilization of the GVBQ targets at extremely low concentration, far surpassing those of most ligands targeting the canonical G4s. This bifunctional peptide conjugate may represent a new approach in manipulating gene activity by targeting GVBQ structures without compromising between specificity and affinity.

MATERIALS AND METHODS

Chemicals, Oligonucleotides, Peptide, DNA, and Plasmid. Custom synthesis of SBED-GMP was purchased from Takara Biotechnology.[21] Pyridostatin (PDS) was purchased from Sigma and NMM from Frontier Scientific. Fluorescently labeled oligonucleotides were purchased from Takara Biotechnology. Other oligonucleotides were purchased from Sangon Biotechnology. GRPC and RHAU23 peptide were purchased from SBS Genetech (Beijing). A pGL3-T7-GVBQ plasmid was constructed[9] by inserting a GVBQ-forming sequence between the Hind III and Nco I sites upstream of the firefly luciferase gene in the pGL3-control plasmid (Promega).

DMS Footprinting. Oligonucleotide (0.05 μM) in 50 mM lithium cacodylate buffer (pH 7.4) containing 40% (w/v) PEG 200 and 50 mM LiCl or KCl was heated at 95 °C for 5 min and then cooled down to room temperature at a rate of 0.03 °C/s. It was then incubated in a 200 μL volume with 0.5 μM GRPC or other compounds on ice for 60 min before being subjected to DMS footprinting as previously described.[21]

RNase T1 Footprinting. Footprinting was carried out as described with modifications.[33] Briefly, 5′-FAM-labeled RNA (0.5 μM) was dissolved in 20 mM Tris−HCl (pH 7.4) buffer containing 0.5 mM EDTA and 75 mM KCl or LiCl in a total volume of 20 μL. Samples were denatured by heating at 95 °C for 5 min, cooled down to 20 °C at a rate of 0.03 °C/s, and then incubated on ice for 10 min. Samples were then digested with 0.4 U RNase T1 (Thermo Scientific) on ice for 20 min, and the reaction was terminated by phenol/chloroform extraction. The digested RNAs were resolved on a 20% urea denaturing polyacrylamide gel and scanned on a Typhoon 9400 Imager (GE Healthcare).

Electrophoresis Mobility Shift Assay (EMSA). EMSA was carried out as described with modifications.[34] 5′-FAM-labeled DNA was dissolved at 10 or 20 nM in a buffer containing 20 mM Tris−HCl (pH 7.4), 50 mM KCl, and 40% (w/v) PEG 200, denatured at 95 °C for 5 min, and slowly cooled down to 20 °C. The DNA was then incubated with the indicated concentration of GRPC in a buffer of 20 mM Tris−HCl (pH 7.4), 50 mM KCl, 40% (w/v) PEG 200, 0.2 mg/mL BSA, and 0.1 mg/mL fish sperm DNA at 4 °C for 1 h. The DNA−GRPC complexes were resolved on a 16% non-denaturing polyacrylamide gel containing 40% (w/v) PEG 200 and 150 mM KCl at 4 °C for 3 h in a 1× TBE buffer containing 150 mM KCl. RNA was prepared as described[34] and then dissolved at 20 nM in a buffer containing 20 mM Tris−HCl (pH 7.4), 75 mM KCl, 0.2 mg/mL BSA, and 0.1 mg/mL yeast tRNA. It was incubated with the indicated concentration of GRPC or RHAU23 before being resolved on gel.

Thermal Melting Profiling by Fluorescence Resonance Energy Transfer (FRET). FRET melting was carried out as previously described.[21]

Microscale Thermophoresis (MST). MST experiments were performed on a Monolith NT.115 system (NanoTemper Technologies) as described.[26,35] FAM-labeled DNA was denatured/renatured as in the EMSA, and then, 100 nM DNA was incubated with the indicated concentration of compound for 60 min at 4 °C in a binding buffer (20 mM Tris−HCl, pH 7.4, 50 mM KCl, 40% (w/v) PEG 200, 0.2 mg/mL BSA, 0.05% Tween-20). The samples were loaded into microscale thermophoresis (MST)-grade glass capillaries. The MST measurement was carried out at 50% blue LED excitation power and 40% infrared power. The MST data analyses were performed using the MO.Affinity Analysis V2.3 software.

Circular Dichroism (CD) Spectroscopy. CD spectroscopy was carried out as previously described.[21]

Photo-Cross-Linking. Photo-cross-linking was carried out as previously described with minor modifications.[21] Briefly, 0.1 μM oligonucleotide was incubated on ice for 30 min with 1 mg/mL fish sperm DNA, 0.5 mM SBED-GMP, and the indicated concentration of GRPC in a buffer of 50 mM lithium cacodylate (pH 7.4) containing 50 mM KCl and 40% (w/v) PEG 200 before being irradiated by UV light. For RNA, fish sperm DNA was replaced by the same concentration of yeast tRNA and 1 U/μL RNase inhibitor.

DNA Polymerase Stop Assay. DNA polymerase stop assay was carried out as described with modifications.[21] Annealed primer and template DNA were incubated with various concentrations of GRPC or RHAU23 peptide on ice for 30 min. Primer extension was initiated by adding a final concentration of 10 mM $MgCl_2$, 50 μM dNTP (Thermo Scientific), and 0.15 U/μL Bsu DNA Polymerase, Large Fragment (NEB). The reactions were kept at 37 °C for 10 min and then stopped by adding 1/20 volume of 0.5 M EDTA−Na_2 (pH 8.0) and heating at 95 °C for 10 min, followed by proteinase K digestion for 30 min at 37 °C. The DNA was extracted with phenol/chloroform and resolved on a denaturing polyacrylamide gel.

Reverse Transcription. A 282 bp linear DNA covering the T7 promoter and the inserted GVBQ motif in the pGL3-T7-GVBQ plasmid was made by PCR using the primer pair 5′-CCTCTGAG-CTATTCCAGAAGTAGTG-3′ and 5′-AACCAGGGCGTATCTC-TTCATAG-3′. To prepare RNA for reverse transcription, 2 μg of amplified DNA was transcribed and purified as previously described.[34]

Reverse transcription was carried out as described.[36] 0.06 μM primer (5′-FAM-TCCATGGTGGCTTATGGATGT-3′) was mixed with 0.05 μM of the RNA transcript in a buffer of 50 mM Tris−HCl (pH 7.4) and 75 mM KCl, denatured at 95 °C for 5 min, and then cooled down to 20 °C at a rate of 0.03 °C/s. The sample was incubated with 1 U/μL RNase Inhibitor and GRPC or another compound on ice for 30 min. RNA reverse transcription was initiated by adding a final concentration of 3 mM $MgCl_2$, 100 μM dNTP (Thermo Scientific), 10 mM DTT, and 1.5 U/μL M-MLV Reverse Transcriptase (Promega). The reactions were kept at 42 °C for 15 min and then stopped by heating at 70 °C for 15 min, followed with proteinase K digestion for 30 min at 37 °C and extracted by phenol/chloroform. DNA product was dissolved in 80% formamide, denatured at 95 °C for 5 min, and resolved on a denaturing polyacrylamide gel. DNA fragments were visualized on a Typhoon Imager (GE Healthcare) and quantitated using the Image Quant 5.2 software.

***In Vitro* Translation and Luciferase Assay.** The pGL3-T7-GVBQ plasmid was linearized by cutting at the BamH I site and purified by the Wizard PCR Clean-Up System (Promega). The linearized plasmid was transcribed as described in the previous section to prepare an RNA template for *in vitro* translation. *In vitro* translation of the RNA was carried out using the Rabbit Reticulocyte Lysate, Nuclease Treated (Promega) according to the manufacturer's instruction. RNA coding firefly luciferase was mixed with RNA coding renilla luciferase and GRPC or the indicated compound in a buffer of 10 mM Tris−HCl (pH 7.4), 75 mM KCl followed by incubation on ice for 30 min. The mixture was then added to the Rabbit Reticulocyte Lysate, and translation was performed at 30 °C for 1 h. Firefly and renilla luciferase activity were measured using the Dual-Luciferase Reporter Assay System (Promega) using the manufacturer's protocol on a Multi-Plate Reader (Biotek, USA).

https://dx.doi.org/10.1021/jacs.0c00774
J. Am. Chem. Soc. 2020, 142, 11394−11403

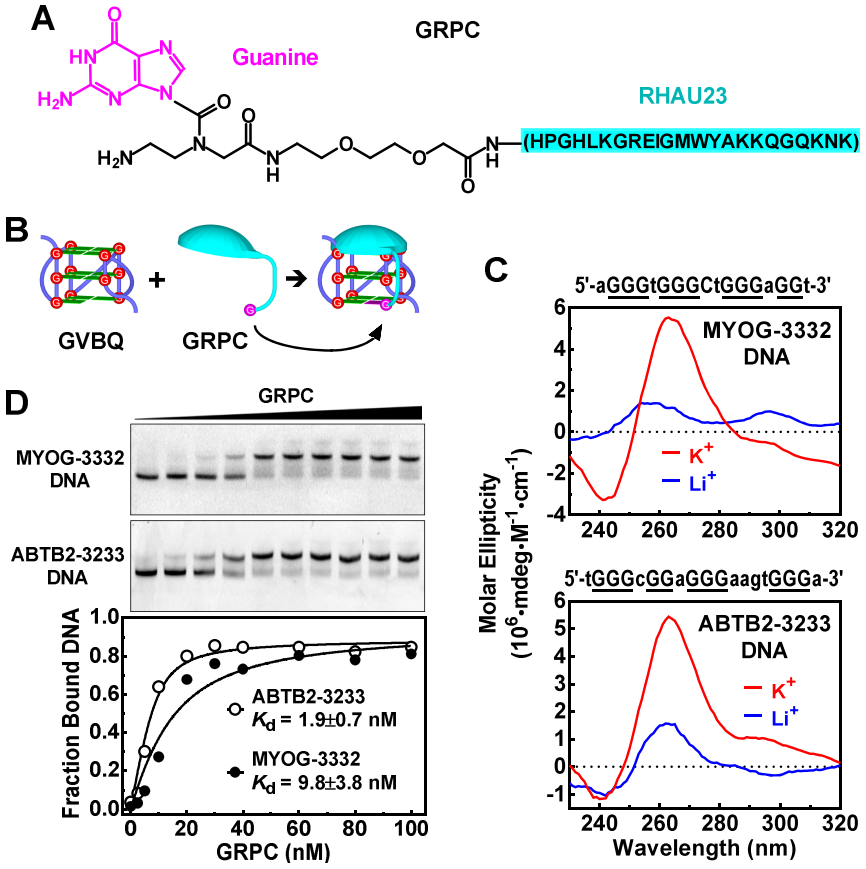

Figure 1. Targeting DNA GVBQs with a guanine−RHAU23 peptide conjugate (GRPC). (A) The GRPC consisting of an RHAU23 peptide covalently linked with a guanine group. (B) Scheme of the expected interaction between GRPC and GVBQ. (C) GVBQ formation in MYOG-3332 and ABTB2-3233 DNA in K^+ or Li^+ solution detected by circular dichroism (CD) spectroscopy. (D) Binding of GRPC to GVBQ detected by electrophoretic mobility shift assay (EMSA).

RESULTS

GRPC Binds DNA GVBQ with High Affinity and Specificity. The bifunctional GRPC was composed of a guanine base and a G4-binding domain (RHAU23) from the RHAU protein (Figure 1A). According to previous studies, the guanine should fill into the G-vacancy of a GVBQ[20,21] and the RHAU23 cap to a G-quartet terminal layer[32] (Figure 1B). We first tested this anticipation with two GVBQ-forming DNAs, i.e., MYOG-3332 and ABTB2-3233 (Table S1), each containing one G_2 and three G_3 tracts in the G-core. The two DNAs form a GVBQ structure with a G-vacancy in one of the guanine terminal layers that can be filled by a guanine residual.[21] The CD spectra of the DNAs in K^+ solution suggested that these two DNAs adopted a parallel folding topology, as indicated by a positive peak at 265 nm and a negative peak at 245 nm (Figure 1C).

We first examined the interaction between the GRPC and the two GVBQs by the electrophoresis mobility shift assay (EMSA). For both DNAs, the amount of DNA−GRPC complex increased in association with an increase in GRPC concentration (Figure 1D), yielding a calculated K_d of 9.8 and 1.9 nM, respectively. The same EMSA was also conducted with two groups of similar DNAs that could either form canonical G4s without a G-vacancy or containing two G_2 tracts (Figure S1). In these cases, the GRPC showed little binding activity to them, demonstrating that the targets of the GRPC were strictly limited to the GVBQ structures. We also tested another nine motifs from human or viral genes (Table S1) that folded into parallel GVBQs (Figure S2) and were bound by the GRPC with nM affinity (Figure S3). The affinity data obtained with EMSA were further verified by the microscale thermophoresis (MST) technique[37] with four representative GVBQ motifs that have a G_2 tract at four alternative positions, respectively (Figure S4). These high-affinity bindings were a result of a synergy between the guanine base and RHAU23 in the GRPC because the individual guanosine and RHAU23 component both showed μM affinity to the MYOG-3332 GVBQ (Figure S5), which was 3 orders of magnitude weaker than that of the GRPC.

G-Vacancy-Dependent Interaction between GRPC and DNA GVBQ. The participation of guanines in the formation of a G4 can be justified by DMS footprinting through the protection of participating guanines from chemical cleavage.[38] Specific to the GVBQ, the guanine in the G-triad facing the G-vacancy is not protected but rather hyper-cleaved.[21] We carried out DMS footprinting to verify the formation of GVBQ in the two DNAs. The formation of GVBQ in the MYOG-3332 in K^+ solution protected the guanine residuals in the G-tracts from chemical cleavage (Figure 2A and B), except for the last one in the first G_3 tract from the 5′ side (red arrowhead) that was instead hypercleaved (green versus red curve). The addition of guanosine and RHAU23 either individually or in combination slightly reduced the hypercleavage, as judged from a small drop of the cleavage peak, suggesting that the two individual compounds had little effect in stabilizing the GVBQs. However, when GRPC was

https://dx.doi.org/10.1021/jacs.0c00774
J. Am. Chem. Soc. 2020, 142, 11394−11403

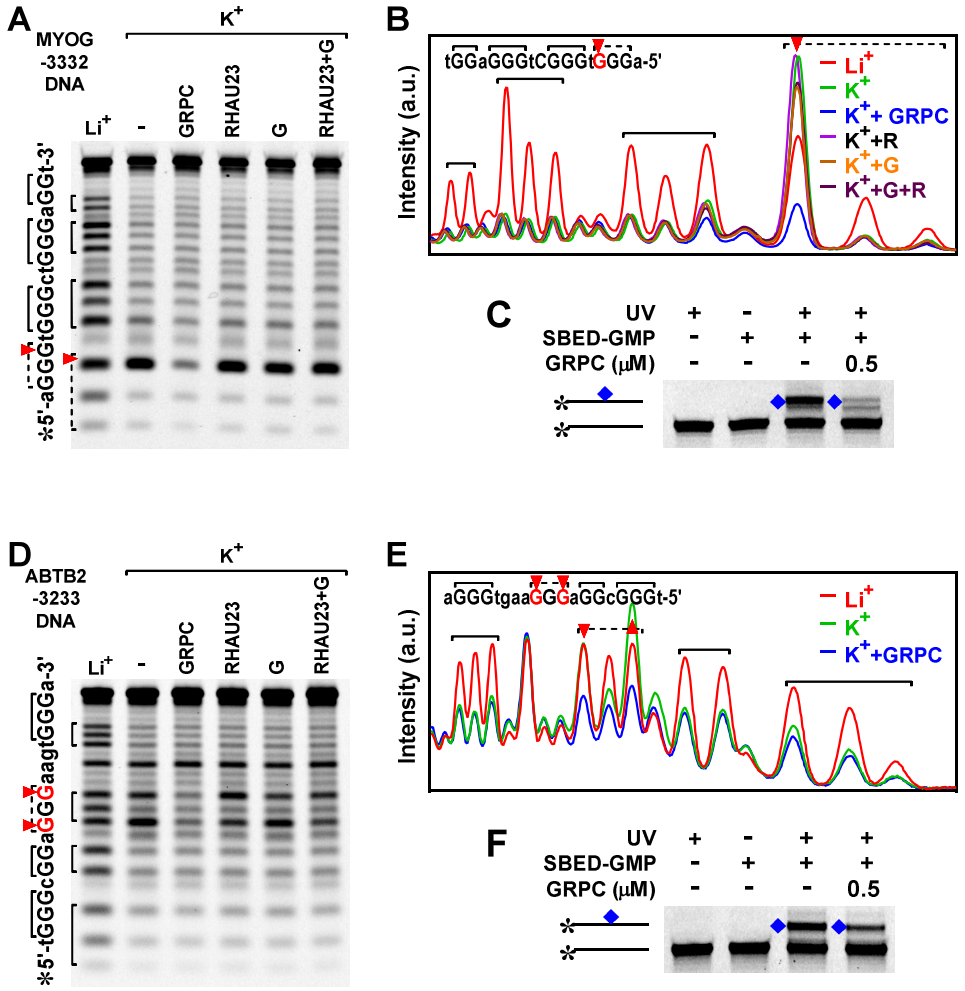

Figure 2. Verification of guanine filling-in in the DNA GVBQ–GRPC interaction. (A) DMS footprinting of MYOG-3332 DNA in the presence of GRPC, RHAU23, guanosine (G), and RHAU23 plus guanosine (RHAU23+G). (B) Digitization of the gel in part A. R, RHAU23; G, guanosine. (C) Competition of GRPC with SBED-GMP in the photo-cross-linking assay. (D–F) Same as parts A–C except the GRPC was tested with ABTB2-3233 DNA.

added, the hypercleavage completely disappeared and the guanine became well protected, as were the other guanines in the G-tracts (blue versus red curve). This result indicated that the G-vacancy in the GVBQ was occupied by the guanine in the GRPC and the GVBQ was effectively stabilized by the joint action of the guanine and RHAU23 moiety.

We further used a photo-cross-linking experiment with a trifunctional compound SBED-GMP to confirm the guanine filling-in.[21] The SBED-GMP carries a guanine moiety to fill in a G-vacancy, a phenyl azide group that can react with a primary amine in adenine, guanine, or cytosine to cross-link a DNA. When a G-vacancy is filled with the guanine base from the SBED-GMP, the two interacting partners can be covalently cross-linked upon UV irradiation. In Figure 2C, it can be seen that such a cross-link occurred in the DNA in the presence of SBED-GMP and UV light (blue diamond), as indicated by an extra DNA band above the original DNA. This extra band was dramatically weakened when GRPC was added, implying that the GRPC and SBED-GMP competed for the G-vacancy. The same set of analyses was carried out with the ABTB2-3233, and the results obtained were fully supportive of the fill-in targeting by the GRPC (Figure 2D–F).

G-Vacancy-Dependent Interaction between GRPC and RNA GVBQ. To explore the possibility of targeting GVBQs in RNA, we also tested two RNA equivalents of the MYOG-3332 and ABTB2-3233 sequences. RNA G4s almost exclusively adopt a parallel conformation.[39] Similar to the corresponding DNAs, the two RNA also formed parallel G4s in K^+ solution, as they both featured a positive peak at 265 and a negative peak at 245 nm (Figure S6A). The formation of G4 in the two RNAs was further confirmed by RNase T1 footprinting in which the guanines participating in G4 formation were protected from cleavage (Figure S6B). Again, the guanine filling-in was also confirmed by the photo-cross-linking experiment in which the GRPC competed with the guanine of the SBED-GMP (Figure S6C). These results illustrated that the GRPC could also target GVBQs in RNAs.

Stabilization of DNA/RNA GVBQs by GRPC. To assess the stabilization of GVBQs by the GRPC, we labeled the DNAs at the 5′ end with a FAM as a donor and the 3′ end with a TAMRA as an acceptor and performed thermal melting based on the fluorescence resonance energy transfer (FRET) technique.[40,41] A GVBQ was incubated with different concentrations of GRPC, and the temperature required for

https://dx.doi.org/10.1021/jacs.0c00774
J. Am. Chem. Soc. 2020, 142, 11394–11403

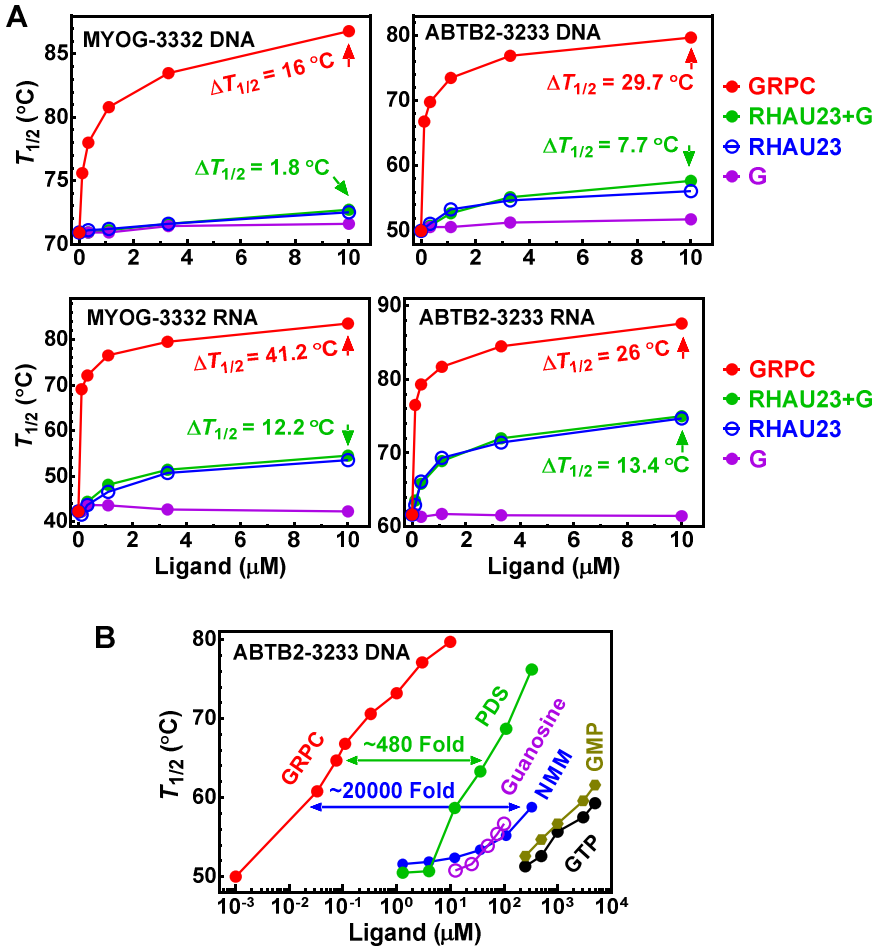

Figure 3. Stabilization of GVBQ DNA and RNA of MYOG-3332 and ABTB2-3233 by GRPC. (A) $T_{1/2}$ of thermal melting of GVBQs in the presence of different concentrations of GRPC. $T_{1/2}$ indicates the temperature for the fluorescence in a FRET melting to reach the midvalue between the minimum and maximum values. (B) Comparison of thermal stabilities of ABTB2-3233 DNA stabilized by GRPC and other compounds.

the fluorescence to reach the midvalue between the minimal and maximal fluorescence, denoted as $T_{1/2}$, was used to judge the stability of the GVBQs. As shown in Figure 3A, the stability of the four GVBQs was enhanced in a positive correlation with the concentration of GRPC. At 10 μM of GRPC, the greatest stabilization occurred to the GVBQ of the MYOG-3332 RNA, resulting in an increase in the $T_{1/2}$ value of 41 °C. At 1 μM, the GRPC enhanced the $T_{1/2}$ value by nearly 30 °C for the MYOG-3332 RNA. In any case, the stabilization with the GRPC was far greater than that with guanosine and RHAU23 added either individually or in combination, indicating a dramatic improvement through the synergy of the two functional units in the GRPC. Moreover, the stabilization involved the G-vacancy in that it only diminished when facing a competition from a GVBQ but not from a canonical G4 (Figure S7).

We also conducted thermal melting experiments using other G4 or GVBQ binding compounds to evaluate the effect of the GRPC (Figure 3B). Among them, the popular G4 stabilizer pyridostatin (PDS)[42] significantly outperformed guanosine, *N*-methyl mesoporphyrin IX (NMM),[43] GMP, and GTP in stabilizing the ABTB2 DNA GVBQ. The PDS was reported to have a K_d value of 490 nM[44] and NMM of ~10 μM[45] to the telomeric G4. With a K_d value of a few nM (Figure 1D), the GRPC was ~480-fold more potent than the PDS and ~20000-fold more potent than the NMM (Figure 3B), not to mention the other stabilizers.

GRPC Inhibits *in Vitro* DNA Replication and RNA Reverse Transcription. Our aforementioned results demonstrated a dramatic improvement in the stabilization of the GVBQs by a guanine-guided targeting. Next, we examined how such targeting would affect DNA replication. Primer extension was performed on a DNA template with a GVBQ in the middle in the absence and presence of different concentrations of GRPC. As shown in Figure 4A (solid circles), the GRPC caused serious premature termination (PT) of replication in front of the two GVBQs (Figure S8) in a concentration-dependent manner, which was in sharp contrast to that caused by the RHAU23 without the guanine guide (open circles). The DNA replication was totally blocked when the GVBQs were replaced by equivalent canonical G4s even in the absence of GRPC such that no effect of GRPC could be observed (Figure 4A, blue curve). This result implied that such G4s were stable enough to fully stall the replication and supported our assumption that stable G4s are not preferred targets. Premature replication termination also remained low in the presence of the ligand PDS and NMM (Figure 4B). Similarly, GRPC mediated premature termination of reverse transcription was also observed at the GVBQs on an RNA template in a concentration-dependent manner (Figure S9).

https://dx.doi.org/10.1021/jacs.0c00774
J. Am. Chem. Soc. 2020, 142, 11394−11403

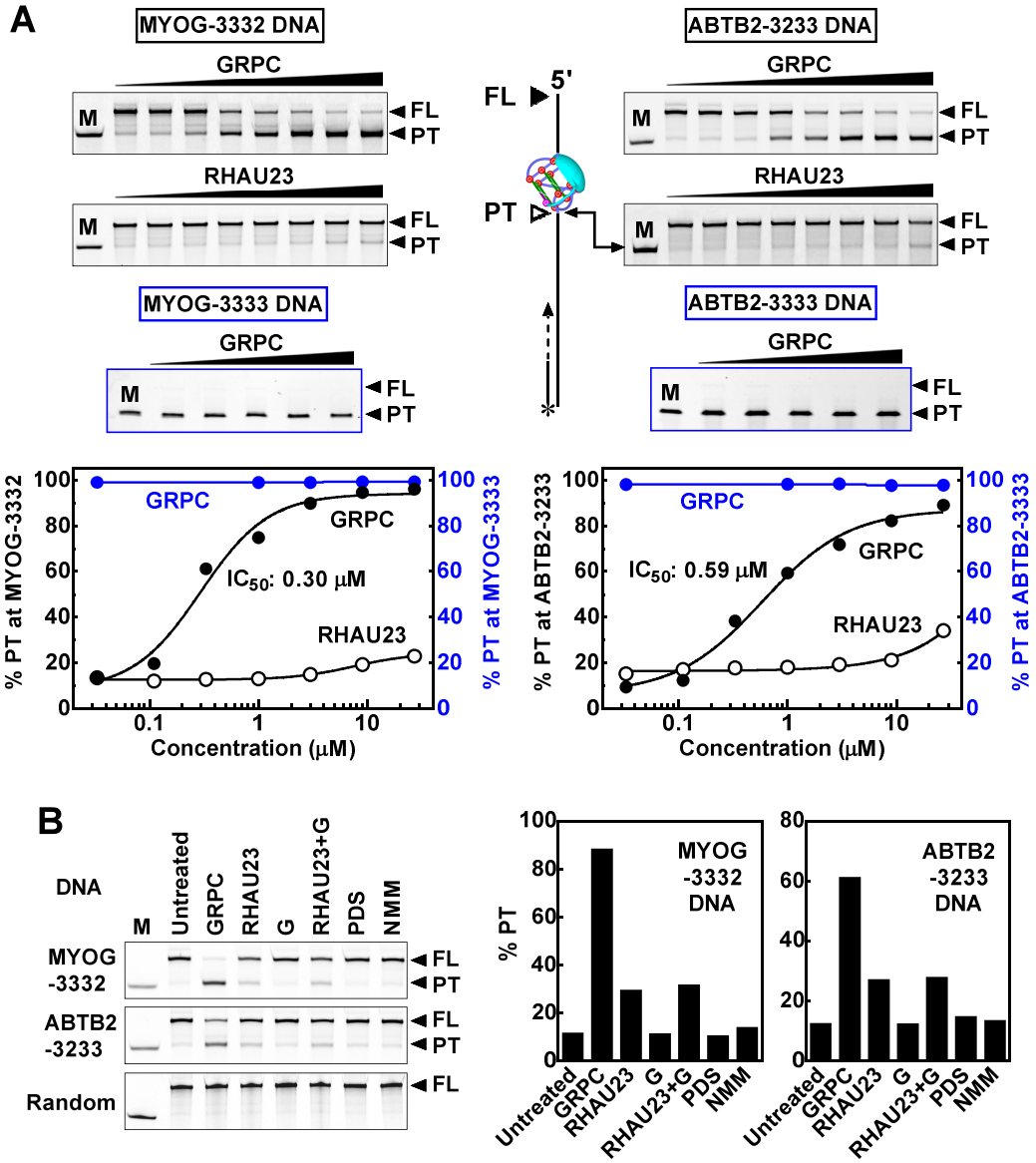

Figure 4. Inhibition of DNA replication by targeting GVBQ with GRPC and other compounds. Primer extension of DNAs containing an MYOG-3332 or ABTB2-3233 GVBQ, or a canonical G4 motif in the middle was conducted in the presence of the indicated compounds. (A) Premature termination (PT) as a function of GRPC or RHAU23 concentration. PT was expressed as a percentage of the total synthesized DNA. (B) Comparison of PT in the presence of 10 μM of the indicated compounds. Marker (M) indicates the mobility of a synthetic DNA complementary to the whole region flanking the 3′ side of the GVBQ on the template.

GRPC Inhibits *in Vitro* RNA Translation. Previous studies have shown that G4s in the 5′ UTR of many human mRNAs generally suppress translation[46,47] and such suppression can be intensified by G4 stabilizers.[48,49] To evaluate the effect of GRPC on RNA GVBQ in this process, we performed *in vitro* translation using RNA templates in which an MYOG-3332 or ABTB2-3233 GVBQ was arranged in the 5′ UTR of a firefly luciferase gene. As is shown in Figure 5A and B, the addition of GRPC remarkably inhibited the reporter activity in the RNA containing GVBQ in a dose-dependent manner, while the RHAU23 alone had little effect and the PDS was much less effective.

We also tested the MYOG-3333 G4 and found GRPC and RHAU23 both inhibited the translation when their concentration reached 10 and 20 μM (Figure 5C). RNA forms rich secondary structures. In this case, the G4 was not stable because it had to compete against such structures. The two compounds might promote the formation of the G4 in the competition to inhibit the translation. The fact that the GRPC was more potent than RHAU23 was intriguing, since it was unexpected because there was no G-vacancy in the MYOG-3333 G4 for the guanine in the GRPC to fill-in. To seek more insight, we assessed the K_d of the interactions (Figure S10). In agreement with the difference in their potency, the GRPC showed a smaller K_d than the RHAU23. However, it was not clear how the guanine in the GRPC improved the affinity. While this phenomenon deserves further investigation, it suggested that targeting RNA may be more complicated than targeting DNA. For the random RNA, a weak inhibition at 20 μM of GRPC and PDS might be caused by the presence of a G4 of two G-quartet layers.

https://dx.doi.org/10.1021/jacs.0c00774
J. Am. Chem. Soc. 2020, 142, 11394−11403

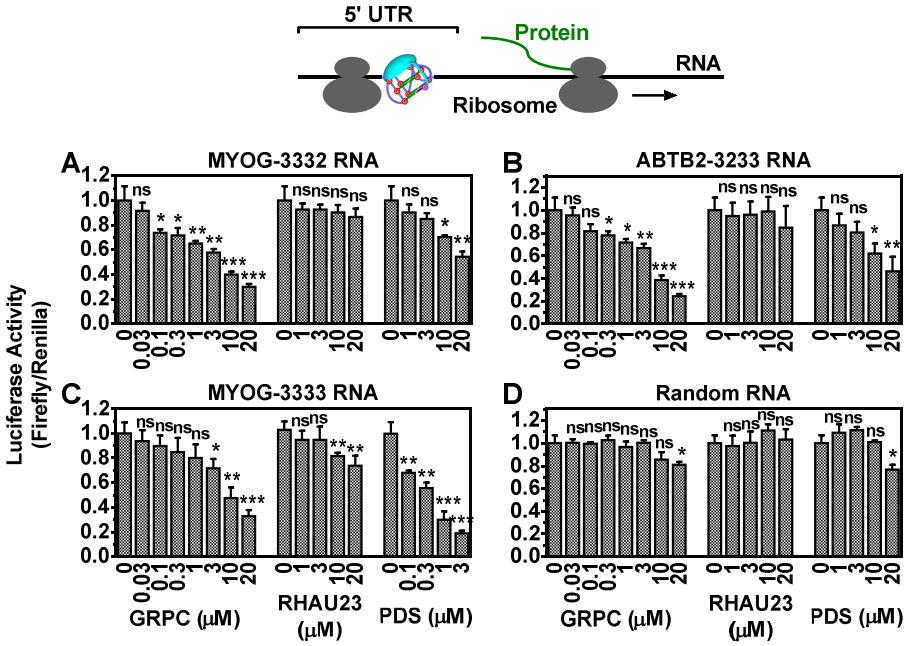

Figure 5. Effect of GRPC on translation with RNA hosting a GVBQ, random, or canonical G4 motif at the 5′-UTR. The translation was conducted in the presence of the indicated compound and quantitated by luciferase reporter activity. Statistical analysis was conducted using an unpaired two-tailed students *t* test (not significant (ns), $P > 0.05$; *, $P < 0.05$; **, $P < 0.01$; ***, $P < 0.001$).

DISCUSSION

As an alternative to small molecule ligands, our work demonstrated that the GRPC benefited from three aspects in establishing a compound−target interaction with excellent specificity and nM affinity. First, the selective filling-in of the guanine into the G-vacancy resulted in extremely high specificity toward DNA GVBQs. Such selectivity outperformed previous ligands in that it solely recognizes the intended GVBQ but not even the canonical G4s. Second, the synergistic action of the RHAU23 and guanine greatly improved affinity to GVBQs. Third, targeting the less stable GVBQ provided larger room for potency.

Accordingly, the GRPC showed strong binding to GVBQs with K_d at the nM level. This affinity is far greater than that of the small molecule ligands to the canonical G4s whose K_d values are among several tens of nM to several tens of μM.[19] For example, the popular commercially available pyridostatin (PDS) has a K_d value of 490 nM[44] and the NMM has a K_d value of ∼10 μM[45] to the telomere G4. The GRPC remarkably outperformed the representative ligands, such as the PDS and NMM, in stabilizing G4 targets. As is shown in Figure 3B, the GRPC was ∼480-fold more effective than the PDS and ∼20000-fold more effective than the NMM in stabilizing the ABTB2 DNA GVBQ. Even though each ligand may have optimal G4 targets, these large differences are likely to maintain if such a possibility is to be considered.

Off-targeting or nonspecificity is an issue that deserves more attention than we currently paid to. When administered into cells, there are numerous chances for a ligand to interact with biomolecules such as proteins in addition to the intended G4 targets. In one of our previous works, we examined how much G4 stabilization by several ligands with high affinity and selectivity to G4s contributed to the inhibition of telomere DNA extension by telomerase.[50] One of the ligands, Zn-TTAPc, a derivative of phthalocyanines, has a K_d to G4 at the nM level, which is hundreds to thousands fold smaller than to tRNA and the corresponding cDNAs.[51] In such assays, the reactants simply included telomerase, NTPs, and DNA substrate that could form G4s. Our results showed that most of the inhibition was G4 irrelevant and G4 stabilization only made a minor or even a negligible contribution to the overall inhibition.

The highly specific targeting of GVBQ by the GRPC holds promise to overcome the off-targeting issue in a cellular environment. In this particular case, the RHAU23 is derived from the original RUAU protein by removing >90% of the amino acid residues such that the chance for the GRPC to interact with other cellular components is minimized. Because the RHAU23 and guanine are both of natural origin, one may expect less cell toxicity from the GRPC, another benefit over the small molecule ligands.

Unlike the small-molecule ligands, the GRPC inherits the weakness of peptide drugs in, for instance, intracellular delivery and metabolic properties.[52−54] The capability of intracellular delivery may be implemented by linking a cell-penetrating peptide (CPP)[55−57] to the GRPC. CCPs are small amino-acid sequences with a size of a few to less than 30 residues that can deliver therapeutic molecules, including DNA, proteins, peptides, and oligonucleotides, into cells. Many CPPs are in preclinical or clinical development and worth being tested with the GRPC. Once delivered into cells, site-specific targeting of a single specific GVBQ of interest may be realized by attaching a PNA (peptide nucleic acid)[58] or LNA (locked nucleic acid)[59] sequence to GRPC to recognize a region flanking the intended GVBQ motif. In addition, the PNA/LNA is expected to enhance the affinity and specificity toward the intended target due to an additional sequence-specific hybridization. The GRPC is also subject to proteolysis in cells. This issue may be overcome by cyclization of RHAU23 that has been reported to confer the RHAU23 superior resistance against exopeptidase.[60]

https://dx.doi.org/10.1021/jacs.0c00774
J. Am. Chem. Soc. 2020, 142, 11394−11403

CONCLUSION

A highly specific and potent strategy for targeting nucleic acids was implemented by linking a guanine group to a G4-binding peptide RHAU23 to specifically guide an interaction toward a distinctive type of G4s carrying a guanine vacancy. The synergistic action of a guided binding and stabilization ensures exclusive recognition of the intended targets with affinities at nM level and capability to intervene in a variety of metabolic activities associated with DNA.

ASSOCIATED CONTENT

Supporting Information

The Supporting Information is available free of charge at https://pubs.acs.org/doi/10.1021/jacs.0c00774.

Figures showing GRPC did not bind MYOG-3333, ABTB2-3333, MYOG-2332, and ABTB2-2233 DNA; GVBQ formation in nine DNAs in K^+ or Li^+ solution detected by CD spectroscopy; dissociation constant K_d of GRPC to nine DNA GVBQs determined by EMSA; dissociation constant K_d values of GRPC to four representative DNA GVBQs determined by MST; dissociation constant K_d of RHAU23 and guanosine to MYOG-3332 DNA GVBQ determined by MST; targeting RNA GVBQ with GRPC; stabilization of fluorescently labeled ABTB2-3233 GVBQ by GRPC in competition with unlabeled ABTB2-3233 GVBQ and ABTB2-3333 G4; primer extension on the DNA template stopped in front of the GVBQ stabilized by GRPC; inhibition of RNA reverse transcription by targeting GVBQ with GRPC and RHAU23; and dissociation constant K_d of GRPC and RHAU23 to MYOG-3333 RNA G4 determined by EMSA and table showing oligonucleotides used in this study (PDF)

AUTHOR INFORMATION

Corresponding Authors

Ke-wei Zheng − *School of Pharmaceutical Sciences (Shenzhen), Sun Yat-Sen University, Guangzhou 510275, P. R. China; State Key Laboratory of Membrane Biology, Institute of Zoology, Chinese Academy of Sciences, Beijing 100101, P. R. China*; Email: zhengkw6@mail.sysu.edu.cn

Zheng Tan − *State Key Laboratory of Membrane Biology, Institute of Zoology, Chinese Academy of Sciences, Beijing 100101, P. R. China; Center for Healthy Aging, Changzhi Medical College, Changzhi 046000, Shanxi, P. R. China*; orcid.org/0000-0003-0480-9686; Email: z.tan@ioz.ac.cn

Authors

Yi-de He − *MOE Key Laboratory of Gene Function and Regulation, School of Life Sciences, Sun Yat-Sen University, Guangzhou 510275, P. R. China; State Key Laboratory of Membrane Biology, Institute of Zoology, Chinese Academy of Sciences, Beijing 100101, P. R. China*

Cui-jiao Wen − *State Key Laboratory of Membrane Biology, Institute of Zoology, Chinese Academy of Sciences, Beijing 100101, P. R. China*

Xin-min Li − *State Key Laboratory of Membrane Biology, Institute of Zoology, Chinese Academy of Sciences, Beijing 100101, P. R. China*

Jia-yuan Gong − *State Key Laboratory of Membrane Biology, Institute of Zoology, Chinese Academy of Sciences, Beijing 100101, P. R. China*

Yu-hua Hao − *State Key Laboratory of Membrane Biology, Institute of Zoology, Chinese Academy of Sciences, Beijing 100101, P. R. China*

Yong Zhao − *MOE Key Laboratory of Gene Function and Regulation, School of Life Sciences, Sun Yat-Sen University, Guangzhou 510275, P. R. China*

Complete contact information is available at: https://pubs.acs.org/10.1021/jacs.0c00774

Notes

The authors declare no competing financial interest.

ACKNOWLEDGMENTS

We thank the National Natural Science Foundation of China for funding K.-w.Z. to initiate this work by grant no. 21708042 and further supporting by grants 21672212 and 21432008. Y.-d.H. was supported by the China Postdoctoral Science Foundation, grant 2019M653167, and Fundamental Research Funds for the Central Universities, grant 19lgpy197.

REFERENCES

(1) Asamitsu, S.; Obata, S.; Yu, Z.; Bando, T.; Sugiyama, H. Recent Progress of Targeted G-Quadruplex-Preferred Ligands Toward Cancer Therapy. *Molecules* **2019**, *24* (3), 429.

(2) Ruggiero, E.; Richter, S. N. G-quadruplexes and G-quadruplex ligands: targets and tools in antiviral therapy. *Nucleic Acids Res.* **2018**, *46* (7), 3270−3283.

(3) Bessi, I.; Wirmer-Bartoschek, J.; Dash, J.; Schwalbe, H. Targeting G-quadruplex with Small Molecules: An NMR View. In *Modern Magnetic Resonance*; Webb, G. A., Ed.; Springer International Publishing: Cham, Switzerland, 2017; pp 1−22.

(4) Zhao, Y.; Du, Z.; Li, N. Extensive selection for the enrichment of G4 DNA motifs in transcriptional regulatory regions of warm blooded animals. *FEBS Lett.* **2007**, *581* (10), 1951−6.

(5) Eddy, J.; Vallur, A. C.; Varma, S.; Liu, H.; Reinhold, W. C.; Pommier, Y.; Maizels, N. G4 motifs correlate with promoter-proximal transcriptional pausing in human genes. *Nucleic Acids Res.* **2011**, *39* (12), 4975−83.

(6) Xiao, S.; Zhang, J. Y.; Zheng, K. W.; Hao, Y. H.; Tan, Z. Bioinformatic analysis reveals an evolutional selection for DNA:RNA hybrid G-quadruplex structures as putative transcription regulatory elements in warm-blooded animals. *Nucleic Acids Res.* **2013**, *41* (22), 10379−90.

(7) Huppert, J. L.; Balasubramanian, S. G-quadruplexes in promoters throughout the human genome. *Nucleic Acids Res.* **2007**, *35* (2), 406−13.

(8) Zhang, C.; Liu, H. H.; Zheng, K. W.; Hao, Y. H.; Tan, Z. DNA G-quadruplex formation in response to remote downstream transcription activity: long-range sensing and signal transducing in DNA double helix. *Nucleic Acids Res.* **2013**, *41* (14), 7144−52.

(9) Zheng, K. W.; He, Y. D.; Liu, H. H.; Li, X. M.; Hao, Y. H.; Tan, Z. Superhelicity Constrains a Localized and R-Loop-Dependent Formation of G-Quadruplexes at the Upstream Region of Transcription. *ACS Chem. Biol.* **2017**, *12* (10), 2609−2618.

(10) Zhao, Y.; Zhang, J. Y.; Zhang, Z. Y.; Tong, T. J.; Hao, Y. H.; Tan, Z. Real-Time Detection Reveals Responsive Cotranscriptional Formation of Persistent Intramolecular DNA and Intermolecular DNA:RNA Hybrid G-Quadruplexes Stabilized by R-Loop. *Anal. Chem.* **2017**, *89* (11), 6036−6042.

(11) Wu, R. Y.; Zheng, K. W.; Zhang, J. Y.; Hao, Y. H.; Tan, Z. Formation of DNA:RNA hybrid G-quadruplex in bacterial cells and its dominance over the intramolecular DNA G-quadruplex in mediating transcription termination. *Angew. Chem., Int. Ed.* **2015**, *54* (8), 2447−51.

(12) Zheng, K. W.; Wu, R. Y.; He, Y. D.; Xiao, S.; Zhang, J. Y.; Liu, J. Q.; Hao, Y. H.; Tan, Z. A competitive formation of DNA:RNA hybrid

G-quadruplex is responsible to the mitochondrial transcription termination at the DNA replication priming site. *Nucleic Acids Res.* **2014**, *42* (16), 10832−44.
(13) Zhang, J. Y.; Zheng, K. W.; Xiao, S.; Hao, Y. H.; Tan, Z. Mechanism and manipulation of DNA:RNA hybrid G-quadruplex formation in transcription of G-rich DNA. *J. Am. Chem. Soc.* **2014**, *136* (4), 1381−90.
(14) Xiao, S.; Zhang, J. Y.; Wu, J.; Wu, R. Y.; Xia, Y.; Zheng, K. W.; Hao, Y. H.; Zhou, X.; Tan, Z. Formation of DNA:RNA hybrid G-quadruplexes of two G-quartet layers in transcription: expansion of the prevalence and diversity of G-quadruplexes in genomes. *Angew. Chem., Int. Ed.* **2014**, *53* (48), 13110−4.
(15) Zheng, K. W.; Xiao, S.; Liu, J. Q.; Zhang, J. Y.; Hao, Y. H.; Tan, Z. Co-transcriptional formation of DNA:RNA hybrid G-quadruplex and potential function as constitutional cis element for transcription control. *Nucleic Acids Res.* **2013**, *41* (10), 5533−41.
(16) Zhang, S.; Wu, Y.; Zhang, W. G-quadruplex structures and their interaction diversity with ligands. *ChemMedChem* **2014**, *9* (5), 899−911.
(17) Vy Thi Le, T.; Han, S.; Chae, J.; Park, H. J. G-quadruplex binding ligands: from naturally occurring to rationally designed molecules. *Curr. Pharm. Des.* **2012**, *18* (14), 1948−72.
(18) Li, Q.; Xiang, J. F.; Yang, Q. F.; Sun, H. X.; Guan, A. J.; Tang, Y. L. G4LDB: a database for discovering and studying G-quadruplex ligands. *Nucleic Acids Res.* **2013**, *41* (D1), D1115−23.
(19) Luedtke, N. W. Targeting G-Quadruplex DNA with Small Molecules. *Chimia* **2009**, *63* (3), 134−139.
(20) Li, X. M.; Zheng, K. W.; Hao, Y. H.; Tan, Z. Exceptionally Selective and Tunable Sensing of Guanine Derivatives and Analogues by Structural Complementation in a G-Quadruplex. *Angew. Chem., Int. Ed.* **2016**, *55* (44), 13759−13764.
(21) Li, X. M.; Zheng, K. W.; Zhang, J. Y.; Liu, H. H.; He, Y. D.; Yuan, B. F.; Hao, Y. H.; Tan, Z. Guanine-vacancy-bearing G-quadruplexes responsive to guanine derivatives. *Proc. Natl. Acad. Sci. U. S. A.* **2015**, *112* (47), 14581−6.
(22) Winnerdy, F. R.; Das, P.; Heddi, B.; Phan, A. T. Solution Structures of a G-Quadruplex Bound to Linear- and Cyclic-Dinucleotides. *J. Am. Chem. Soc.* **2019**, *141* (45), 18038−18047.
(23) Heddi, B.; Martin-Pintado, N.; Serimbetov, Z.; Kari, T. M.; Phan, A. T. G-quadruplexes with (4n - 1) guanines in the G-tetrad core: formation of a G-triad.water complex and implication for small-molecule binding. *Nucleic Acids Res.* **2016**, *44* (2), 910−6.
(24) Mukundan, V. T.; Phan, A. T. Bulges in G-quadruplexes: broadening the definition of G-quadruplex-forming sequences. *J. Am. Chem. Soc.* **2013**, *135* (13), 5017−28.
(25) Wu, G.; Xing, Z.; Tran, E. J.; Yang, D. DDX5 helicase resolves G-quadruplex and is involved in MYC gene transcriptional activation. *Proc. Natl. Acad. Sci. U. S. A.* **2019**, *116* (41), 20453−20461.
(26) Wang, K. B.; Dickerhoff, J.; Wu, G.; Yang, D. PDGFR-beta Promoter Forms a Vacancy G-Quadruplex that Can Be Filled in by dGMP: Solution Structure and Molecular Recognition of Guanine Metabolites and Drugs. *J. Am. Chem. Soc.* **2020**, *142* (11), 5204−5211.
(27) Sun, Z. Y.; Wang, X. N.; Cheng, S. Q.; Su, X. X.; Ou, T. M. Developing Novel G-Quadruplex Ligands: from Interaction with Nucleic Acids to Interfering with Nucleic Acid(−)Protein Interaction. *Molecules* **2019**, *24* (3), 396.
(28) Sabater, L.; Nicolau-Travers, M. L.; De Rache, A.; Prado, E.; Dejeu, J.; Bombarde, O.; Lacroix, J.; Calsou, P.; Defrancq, E.; Mergny, J. L.; Gomez, D.; Pratviel, G. The nickel(II) complex of guanidinium phenyl porphyrin, a specific G-quadruplex ligand, targets telomeres and leads to POT1 mislocalization in culture cells. *JBIC, J. Biol. Inorg. Chem.* **2015**, *20* (4), 729−38.
(29) Zhou, G.; Liu, X.; Li, Y.; Xu, S.; Ma, C.; Wu, X.; Cheng, Y.; Yu, Z.; Zhao, G.; Chen, Y. Telomere targeting with a novel G-quadruplex-interactive ligand BRACO-19 induces T-loop disassembly and telomerase displacement in human glioblastoma cells. *Oncotarget* **2016**, *7* (12), 14925−39.
(30) Liu, J. Q.; Chen, C. Y.; Xue, Y.; Hao, Y. H.; Tan, Z. G-quadruplex hinders translocation of BLM helicase on DNA: a real-time fluorescence spectroscopic unwinding study and comparison with duplex substrates. *J. Am. Chem. Soc.* **2010**, *132* (30), 10521−7.
(31) Han, H.; Hurley, L. H.; Salazar, M. A DNA polymerase stop assay for G-quadruplex-interactive compounds. *Nucleic Acids Res.* **1999**, *27* (2), 537−42.
(32) Heddi, B.; Cheong, V. V.; Martadinata, H.; Phan, A. T. Insights into G-quadruplex specific recognition by the DEAH-box helicase RHAU: Solution structure of a peptide-quadruplex complex. *Proc. Natl. Acad. Sci. U. S. A.* **2015**, *112* (31), 9608−13.
(33) Liu, X.; Ishizuka, T.; Bao, H. L.; Wada, K.; Takeda, Y.; Iida, K.; Nagasawa, K.; Yang, D.; Xu, Y. Structure-Dependent Binding of hnRNPA1 to Telomere RNA. *J. Am. Chem. Soc.* **2017**, *139* (22), 7533−7539.
(34) Liu, H. H.; Zheng, K. W.; He, Y. D.; Chen, Q.; Hao, Y. H.; Tan, Z. RNA G-quadruplex formation in defined sequence in living cells detected by bimolecular fluorescence complementation. *Chem. Sci.* **2016**, *7* (7), 4573−4581.
(35) Baaske, P.; Wienken, C. J.; Reineck, P.; Duhr, S.; Braun, D. Optical thermophoresis for quantifying the buffer dependence of aptamer binding. *Angew. Chem., Int. Ed.* **2010**, *49* (12), 2238−41.
(36) Hagihara, M.; Yamauchi, L.; Seo, A.; Yoneda, K.; Senda, M.; Nakatani, K. Antisense-induced guanine quadruplexes inhibit reverse transcription by HIV-1 reverse transcriptase. *J. Am. Chem. Soc.* **2010**, *132* (32), 11171−8.
(37) Moon, M. H.; Hilimire, T. A.; Sanders, A. M.; Schneekloth, J. S., Jr. Measuring RNA-Ligand Interactions with Microscale Thermophoresis. *Biochemistry* **2018**, *57* (31), 4638−4643.
(38) Sun, D.; Hurley, L. H. Biochemical techniques for the characterization of G-quadruplex structures: EMSA, DMS footprinting, and DNA polymerase stop assay. *Methods Mol. Biol.* **2010**, *608*, 65−79.
(39) Fay, M. M.; Lyons, S. M.; Ivanov, P. RNA G-Quadruplexes in Biology: Principles and Molecular Mechanisms. *J. Mol. Biol.* **2017**, *429* (14), 2127−2147.
(40) Zheng, K. W.; Chen, Z.; Hao, Y. H.; Tan, Z. Molecular crowding creates an essential environment for the formation of stable G-quadruplexes in long double-stranded DNA. *Nucleic Acids Res.* **2010**, *38* (1), 327−38.
(41) De Cian, A.; Guittat, L.; Kaiser, M.; Sacca, B.; Amrane, S.; Bourdoncle, A.; Alberti, P.; Teulade-Fichou, M. P.; Lacroix, L.; Mergny, J. L. Fluorescence-based melting assays for studying quadruplex ligands. *Methods* **2007**, *42* (2), 183−95.
(42) Rodriguez, R.; Muller, S.; Yeoman, J. A.; Trentesaux, C.; Riou, J. F.; Balasubramanian, S. A novel small molecule that alters shelterin integrity and triggers a DNA-damage response at telomeres. *J. Am. Chem. Soc.* **2008**, *130* (47), 15758−9.
(43) Ren, J.; Chaires, J. B. Sequence and structural selectivity of nucleic acid binding ligands. *Biochemistry* **1999**, *38* (49), 16067−75.
(44) Koirala, D.; Dhakal, S.; Ashbridge, B.; Sannohe, Y.; Rodriguez, R.; Sugiyama, H.; Balasubramanian, S.; Mao, H. A single-molecule platform for investigation of interactions between G-quadruplexes and small-molecule ligands. *Nat. Chem.* **2011**, *3* (10), 782−7.
(45) Nicoludis, J. M.; Barrett, S. P.; Mergny, J. L.; Yatsunyk, L. A. Interaction of human telomeric DNA with N-methyl mesoporphyrin IX. *Nucleic Acids Res.* **2012**, *40* (12), 5432−47.
(46) Song, J.; Perreault, J. P.; Topisirovic, I.; Richard, S. RNA G-quadruplexes and their potential regulatory roles in translation. *Translation (Austin)* **2016**, *4* (2), No. e1244031.
(47) Bugaut, A.; Balasubramanian, S. 5′-UTR RNA G-quadruplexes: translation regulation and targeting. *Nucleic Acids Res.* **2012**, *40* (11), 4727−41.
(48) Katsuda, Y.; Sato, S.; Asano, L.; Morimura, Y.; Furuta, T.; Sugiyama, H.; Hagihara, M.; Uesugi, M. A Small Molecule That Represses Translation of G-Quadruplex-Containing mRNA. *J. Am. Chem. Soc.* **2016**, *138* (29), 9037−40.
(49) Jodoin, R.; Carrier, J. C.; Rivard, N.; Bisaillon, M.; Perreault, J. P. G-quadruplex located in the 5′UTR of the BAG-1 mRNA affects

https://dx.doi.org/10.1021/jacs.0c00774
J. Am. Chem. Soc. 2020, 142, 11394−11403

both its cap-dependent and cap-independent translation through global secondary structure maintenance. *Nucleic Acids Res.* **2019**, *47* (19), 10247−10266.
(50) Chen, C. Y.; Wang, Q.; Liu, J. Q.; Hao, Y. H.; Tan, Z. Contribution of telomere G-quadruplex stabilization to the inhibition of telomerase-mediated telomere extension by chemical ligands. *J. Am. Chem. Soc.* **2011**, *133* (38), 15036−44.
(51) Alzeer, J.; Luedtke, N. W. pH-mediated fluorescence and G-quadruplex binding of amido phthalocyanines. *Biochemistry* **2010**, *49* (20), 4339−48.
(52) Tesauro, D.; Accardo, A.; Diaferia, C.; Milano, V.; Guillon, J.; Ronga, L.; Rossi, F. Peptide-Based Drug-Delivery Systems in Biotechnological Applications: Recent Advances and Perspectives. *Molecules* **2019**, *24* (2), 351.
(53) Fosgerau, K.; Hoffmann, T. Peptide therapeutics: current status and future directions. *Drug Discovery Today* **2015**, *20* (1), 122−8.
(54) Henninot, A.; Collins, J. C.; Nuss, J. M. The Current State of Peptide Drug Discovery: Back to the Future? *J. Med. Chem.* **2018**, *61* (4), 1382−1414.
(55) Guidotti, G.; Brambilla, L.; Rossi, D. Cell-Penetrating Peptides: From Basic Research to Clinics. *Trends Pharmacol. Sci.* **2017**, *38* (4), 406−424.
(56) Gait, M. J.; Arzumanov, A. A.; McClorey, G.; Godfrey, C.; Betts, C.; Hammond, S.; Wood, M. J. A. Cell-Penetrating Peptide Conjugates of Steric Blocking Oligonucleotides as Therapeutics for Neuromuscular Diseases from a Historical Perspective to Current Prospects of Treatment. *Nucleic Acid Ther.* **2019**, *29* (1), 1−12.
(57) Habault, J.; Poyet, J. L. Recent Advances in Cell Penetrating Peptide-Based Anticancer Therapies. *Molecules* **2019**, *24* (5), 927.
(58) Muangkaew, P.; Vilaivan, T. Modulation of DNA and RNA by PNA. *Bioorg. Med. Chem. Lett.* **2020**, *30* (9), 127064.
(59) Ishige, T.; Itoga, S.; Matsushita, K. Chapter Two - Locked Nucleic Acid Technology for Highly Sensitive Detection of Somatic Mutations in Cancer. In *Advances in Clinical Chemistry*; Makowski, G. S., Ed.; Elsevier: 2018; Vol. *83*, pp 53−72.
(60) Ngo, K. H.; Yang, R.; Das, P.; Nguyen, G. K. T.; Lim, K. W.; Tam, J. P.; Wu, B.; Phan, A. T. Cyclization of a G4-specific peptide enhances its stability and G-quadruplex binding affinity. *Chem. Commun. (Cambridge, U. K.)* **2020**, *56* (7), 1082−1084.

https://dx.doi.org/10.1021/jacs.0c00774
J. Am. Chem. Soc. 2020, 142, 11394−11403